A Low Cost USV for Aqua Farm Inspection

Ottar L. Osen*, Albert Havnegjerde†, Vegard Kamsvåg‡, Sveinung Liavaag§, and Robin T. Bye¶
Software and Intelligent Control Engineering Laboratory
Faculty of Engineering and Natural Sciences
Norwegian University of Science and Technology
NTNU in Ålesund, Postboks 1517, NO-6025 Ålesund, Norway
Email: *ottar.l.osen@ntnu.no, †alberthavnegjerde@live.com, ‡vegardkamsvaag@gmail.com,
§sveinungliavaag@gmail.com ¶robin.t.bye@ntnu.no

***Abstract*—This paper describes the rapid prototyping of a low cost remotely controlled unmanned surface vessel (USV) intended for inspection of aqua farms. There is an increased focus on inspection of ocean-based aqua farms due to three major challenges: escaping fish, sea lice, and algae. Escaping fish may bring diseases to other fish or interbreed with wild fish and damage their gene material. Sea lice is a parasite that may seriously damage the fish, lower its food quality, and if not treated, can spawn and multiply into an epidemic. Finally, algae blooms may lower oxygen levels and kill the fish. To proactively counter these challenges, aqua farm operators need to regularly inspect the fish cages for holes, the water for algae, and the fish for sea lice. Modern ocean-based aqua farms are usually constructed with two rows of sea cages separated by a gangway in the middle, often with a small operation and machinery building at one end. Staff visually inspect the cages from above and from the nearside by walking up and down the gangway. Inspection of the outer side of a cage will normally require a boat with a human inspector on board, whereas subsea inspection will normally require a human diver. Here, we propose a USV design solution for this kind of inspection that provides the aqua farm operator with a remotely controlled unmanned boat and subsea video feed. A working prototype has been designed in less than six months and successfully tested at sea.**

***Index Terms*—USV; ROV; dynamic positioning; low cost; commercial off-the-shelf; rapid prototyping; aquaculture.**

I. Introduction

For many years, the Norwegian University of Science and Technology at campus NTNU in Ålesund (formerly Aalesund University College) has had a strong marine and maritime focus in both research and education. Working closely with the maritime industry, we have extensive experience in providing professional training for the operation of advanced dynamic positioning (DP) systems for mariners, whilst our research and engineering courses in fields such as automation, mechatronics, power systems, and product-, system-, and ship design are all tailored toward the current needs of this industry. Likewise, over the years, our university has maintained close relationships both with the marine industry and Norwegian authorities, investigating marine environmental issues such as the health of fish in aqua farms, sea lice on salmon, the effect of chemicals on aquatic organisms, and the spread of pathogen in Norwegian fjords. Building on the strong in-house maritime and marine competence, we at the Software and Intelligent Control Engineering (SoftICE) Laboratory[1] have identified a need for a low cost remotely controlled USV for aqua farm inspection as a means to counter three major challenges faced by aqua farm operators today, namely escaping fish, sea lice, and algae. Such a USV could supplement or even replace manual inspection, looking for holes in the sea cages, examining the water for algae, and the fish for sea lice, thus enabling the aqua farm operators to be proactive and catching such problems early.

To offer an attractive alternative to manual inspection, we suggest that a USV for aqua farm inspection should have at least the following properties:

- low cost
- small
- silent
- easy to handle
- remotely controlled
- enclosed thrusters
- highly manoeuvrable
- able to carry instruments or payloads
- employ a DP system for stationkeeping

Whilst our proposed USV design solution is targeted towards the application domain of aqua farms, we wish to emphasise that our solution can be seen as a general DP platform with a wide range of purposes in other marine domains.

In the following, we describe the rapid development of a first prototype of the USV, which was part of the bachelor thesis project of co-authors Albert Havnegjerde, Vegard Kamsvåg, Sveinung Liavaag during the spring semester 2016 at NTNU in Ålesund. Videos of the working prototype operating in manual mode (surge, sway, and yaw control)[2] and DP mode[3] are available on YouTube.

II. USV Prototype Design

A USV as a platform for aquaculture inspection will have an operating profile that favours stationkeeping capabilities over speed. Typically the USV will operate in two modes, relocation and inspection. During relocation, the USV must move silently and carefully short distances (50–100 metres) from cage to cage to avoid scaring the fish and harming cage frames or nets. During inspection, the USV must be kept fixed (DP) relative to the sea cage of interest to enable proper investigation.

Each sea cage may contain as much as 200 thousands salmon with a total biomass of 1000 tonnes. Typically about 10 cages are grouped together in a cluster, often with a common walkway, operation cabin and feeding equipment. Hence, it is extremely important that the USV does not pose any threat to the integrity of the sea cages or the rest of the infrastructure. By keeping both the weight and the operating

[1]SoftICE lab website: http://blog.hials.no/softice

[2]USV manual mode: https://youtu.be/SPX4p46UJx0

[3]USV DP mode: https://youtu.be/1R7KdC8L5lY

speed of the USV low, the vessel will pose little to no threat to the installation due to its small momentum. However, propulsion machinery may pose a serious threat to the nets unless proper design choices are made, and a rupture could have serious economic and environmental consequences.

A. Hull

Since stationkeeping is of primary concern, the chosen hull design should yield excellent stationkeeping capabilities, whilst high speed ability is of little or no interest for our application. Corfield and Young [1] found that compared to other vessel types, a catamaran vessel requires more transverse force for stationkeeping. A rigid-hulled inflatable boat (RIB), on the other hand, is less influenced by currents but more from wind. Finally, a regular displacement hull requires less transverse force than a catamaran but more than a RIB. In order to reduce the influence from wind it is important to reduce the boat volume, and especially the height of the superstructure. For better stationkeeping performance, a small-waterplane-area twin hull (SWATH) boat or a semi-submersible boat can be chosen due to the reduced area in the waterline, with less impact from waves. Notably, SWATH and semi-submersible designs are very sensitive to load changes but that may be of minor concern for our application. However, in order to reduce cost and development time for the prototype we chose to limit ourselves to a low cost off-the-shelf (COTS) solution. Specifically, for a first prototype, we chose an 8-feet long, 54 kg, rotation-molded polypropylene boat with dimensions 242×132 cm^2 (length $\times$ width), namely the Pioner 8 Mini (see Fig. 1). Although the boat is only about 8 feet long, its

Fig. 1. Pioner 8 Mini. Image courtesy of Pioner Boats.

dead-weight (loading capacity) is quite high, with the ability to easily hold two adult persons while maintaining a high level of directional stability.

A major reason for our choice of boat is that its polypropylene material can easily be welded. Since the dinghy has a rather flat bottom, its stationkeeping properties will be somewhere between a RIB and a displacement hull. Our choice offers a good compromise between performance and cost and is well suited for rapid prototyping.

B. Thrusters

1) Tunnels and placements: In order to prevent damage to the cage nets it is imperative that all propellers are inside a housing that prevents the propellers from coming in contact with the nets. We need at least as many actuators as the number of degrees of freedom (DOF) we want to control (simultaneously) [2]. Hence, in our case we need at least three actuators for DP in the horizontal plane, controlling surge (forward/backward movement), sway (sideways movement) and yaw (heading). Thrusters with variable heading (compass thrusters, azimuth thrusters) were considered but were depreciated in favour of a simple solution with T200 thrusters by Blue Robotics placed inside tunnels manufactured by Side-Power [3] that contain fewer moving parts and less modifications to the hull.

In order to control sway without affecting the heading, two side thrusters inside tunnels were added to the vessel, one at the bow and one at the stern. For maximum torque when turning (yaw control), the thruster tunnels should be placed as far from the rotation centre of the vessel as possible. Moreover, to get optimal force from the propellers it is important to get them well into the water. The deeper the thrusters are positioned the less they are affected by the waves on the surface, the risk of sucking air is reduced, and the increased water pressure gives better propeller efficiency [3]. Likewise, it is of importance to have an optimal length of the thruster tunnels. A homogeneous directed flow of water advocates a long tunnel, whilst friction advocates a short tunnel. According to the thruster manufacturer, a tunnel length of 2–4 times the diameter is recommended, whereas tunnels longer than 6–7 times the diameter will give reduced performance due to friction [3].

Due to the hydrodynamical properties of water, the effect of these side thrusters will decrease significantly if the vessel is moving forward with speed. Therefore, the chosen side thrusters are good for stationkeeping but they are not a good choice for changing heading when the vessel is in relocation mode. A possible solution is similar to that found on traditional vessels, namely employing either a main propulsor with a rudder, or an azimuth thruster (like an outboard engine). In order to adhere to our principle of as few moving parts as possible and to increase forward thrust, we chose to have two main propulsors for surge and yaw control, mounted in parallel at equal distance of the long-ship centre axis. This gives better manoeuvrability since heading may be adjusted by throttling these thrusters differently. Another big advantage of having two main propulsors instead of one is that we get redundancy, with the number of actuators being greater than the DOFs to be controlled. In stationkeeping mode the main propulsors can assist the side thrusters in changing heading by throttling them in opposite directions, whereas in relocation mode, the added main propulsor provides redundancy and extra thrust for forward motion.

The placement of the four thrusters are shown in a 3D model as well as the real physical prototype in Figs. 2–3. It is obvious that this placement is suboptimal with respect to forward speed due to the huge drag created by the tubes but for operating the USV at low speeds this is acceptable. Due to the dinghy's geometry and the fact that it protrudes only a few centimetres into the water, it is impossible to integrate the tunnels into the hull, which was one of several options we considered.

2) Power requirements: Power requirements for the thrusters are hard to estimate. Although there are methods to

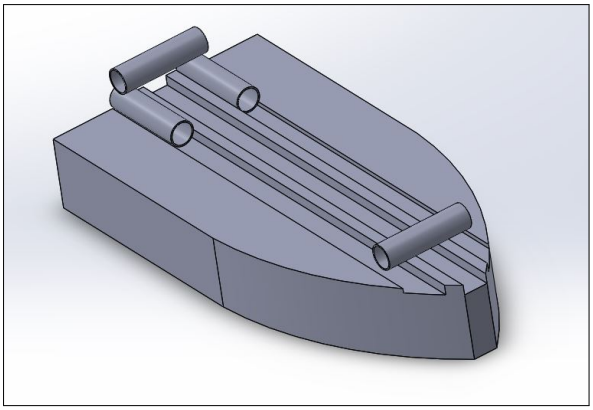

Fig. 2. 3D model of placement of thrusters.

Fig. 3. Placement of thrusters on physical prototype.

find the hull resistance using a towing tank [4], analytically using CFD models, or empirically using the Holtrop and Mennen method [5], they all require accurate models of the vessel and/or facilities that we do not have. Hence, we can only resort to an educated guess for our prototype.

Commercial off-the-shelf (COTS) thrusters suited for our application are quite limited but although a bit small, the T200 thrusters produced by Blue Robotics were chosen for our prototype. These thrusters have become quite popular for remotely operated vehicles (ROVs). According to the manufacturer, these thrusters can produce 34.8N @ 12V and 50N @ 16V. Their propeller efficiency curve (thrust versus power) is depicted in Fig. 4.

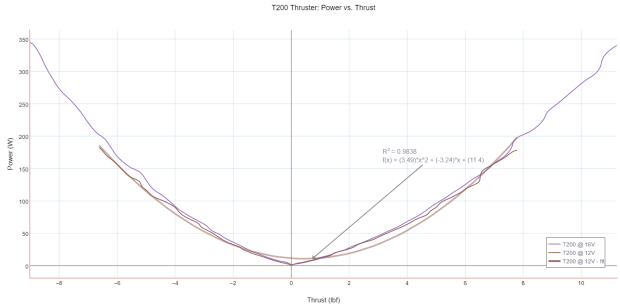

Fig. 4. T200 thrust vs. power [6]

An alternative thruster could have been an electric trolling motor. These are small electric outboard motors and have a thrust of 200–250 N at 12 V and up to 500 N at 36 V. A well-known major producer of these motors are MINN KOTA [7]. However, these motors are significantly more expensive than the T200 and would require more re-engineering to fit our purpose. Hence, we decided to use and test the T200 for this first prototype.

III. Control

A. Dynamic Positioning (DP)

1) DP systems: DP systems are standard on advanced vessels ranging from offshore stand-by-vessels, offshore construction vessels, and rigs to cruise liners. Normally these systems are specialised and expensive equipment containing both advanced sensors and software. The DP system together with the vessel thrusters will allow the vessel to maintain its position and heading down to one meter accuracy within a weather window limited by the vessel's propulsion capacity. A typical DP control system is shown schematically in Fig. 5 [8].

Generally, the DP system will gather information about the vessel's movement, its position and orientation, and the environment, combine this information with a hydrodynamical model of the vessel, and calculate a set of control commands to the thrusters in order to produce the correct force vector that will counteract the external forces and keep the vessel at its desired setpoint and heading [9].

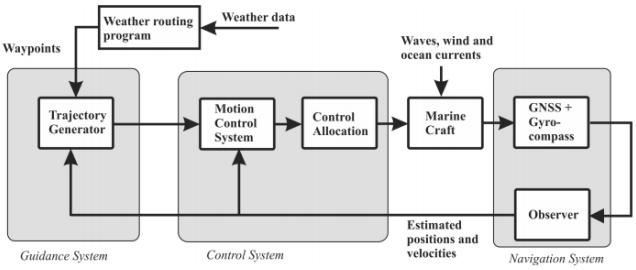

Fig. 5. DP control system (adapted from [8]).

There exists a range of hydrodynamic models for vessels with varying complexity [2]. Models for marine craft are nonlinear due to hydrodynamic forces that are a function of speed, the Coriolis effect, rotation between the body-fixed reference frame (BODY) and global coordinates, and buoyancy forces.

2) Modelling: According to [2], a complex model in 6 DOF of marine craft equations of motion can be represented in vectorial setting as shown in eq. (1) and eq. (2), where $\mathbf{J}_\Theta(\boldsymbol{\eta})$ is a transformation matrix and $\boldsymbol{\eta}$ is the generalised position (displacements and rotations) in 6 DOF. $\boldsymbol{\nu}$ is the generalised vessel velocity, $\boldsymbol{\nu}_c$ is the ocean current velocity, and $\boldsymbol{\nu}_r = \boldsymbol{\nu} - \boldsymbol{\nu}_c$ is the vessel velocity relative to the current velocity, all in 6 DOF. Symbols $\mathbf{M}$, $\mathbf{C}$, and $\mathbf{D}$ represent inertial, Coriolis-centripetal, and damping forces, respectively. The symbol $\boldsymbol{\tau}$ is a vector of forces and moments or the generalized forces in 6 DOF, while $\mathbf{g}(\boldsymbol{\eta})$ is a vector of generalised gravitational and buoyancy forces. The term $\mathbf{g}_0$ represents static restoring forces and moments due to ballast systems and water tanks.

$$\dot{\boldsymbol{\eta}} = \mathbf{J}_\Theta(\boldsymbol{\eta})\boldsymbol{\nu} \tag{1}$$

$$\underbrace{\mathbf{M}_{RB}\dot{\boldsymbol{\nu}} + \mathbf{C}_{RB}(\boldsymbol{\nu})\boldsymbol{\nu}}_{rigid-body\ forces} + \underbrace{\mathbf{M}_A\dot{\boldsymbol{\nu}}_r + \mathbf{C}_A(\boldsymbol{\nu}_r)\boldsymbol{\nu}_r + \mathbf{D}(\boldsymbol{\nu}_r)\boldsymbol{\nu}_r}_{hydrodynamic\ forces} + \underbrace{\mathbf{g}(\boldsymbol{\eta}) + \mathbf{g}_0}_{hydrostatic\ forces} = \boldsymbol{\tau} + \boldsymbol{\tau}_{wind} + \boldsymbol{\tau}_{waves} \tag{2}$$

Due to the complexity of these equations they are mostly used for simulations of vessel dynamics. For control system design a simplification is needed [2].

A linearised model of the vessel in 3 DOF expressed in vessel parallel coordinates may be derived from the nonlinear model based on the following conditions being met [2]:

- low speed (< 2 m/s)
- symmetric vessel (starboard and port halves of the vessel are identical)
- roll (ϕ) and pitch (θ) are small

The linearized model given by [2] is shown in eq. (3), eq. (4) and eq. (5):

$$\dot{\boldsymbol{\eta}}_p = \boldsymbol{\nu} \tag{3}$$

$$(\mathbf{M}_{RB} + \mathbf{M}_A)\dot{\boldsymbol{\nu}} + \mathbf{D}\boldsymbol{\nu} = \mathbf{R}^T(\psi)\mathbf{b} + \boldsymbol{\tau} + \boldsymbol{\tau}_{\text{wind}} + \boldsymbol{\tau}_{\text{wave}} \tag{4}$$

$$\dot{\mathbf{b}} = \mathbf{0} \tag{5}$$

where

$$\boldsymbol{\tau} = \mathbf{T}\mathbf{u} \tag{6}$$

$\mathbf{R}^T(\psi)$ is a transformation matrix and ocean currents are treated as a slowly varying bias vector $\mathbf{b}$. This model is suited for control design and the feedback will compensate for uncertainties in the model. The control matrix $\mathbf{T}$ describe the thruster configuration and $\mathbf{u}$ is the control input vector. Position reference signals $\boldsymbol{\eta}$ are transformed to vessel parallel coordinates at every sample [2].

3) PID control: In DP mode, the geodesic coordinates of the reference point (setpoint) is the origin in the north-east-down (NED) coordinate system frame. The vessel's global positioning system (GPS) coordinates is then converted into coordinates in this NED frame. Hence, these coordinates equals the errors in the north (N) and east (E) directions. Likewise there is a reference heading and a vessel heading. These errors can be fed into a proportional-integral-derivative (PID) controller. The PID controller calculates the required force that must act on the USV in the N and E directions and the rotation torque required to correct the heading. This force vector must be transformed into BODY coordinates. The thrust allocation calculates the thrust needed for every thruster based on the output from the PID controller.

The algorithm can be summarised as follows:

1. Read geodesic coordinates from GPS
2. Read heading from inertial measurement unit (IMU)
3. Transform geodesic coordinates to NED coordinates
4. Calculate heading error
5. Calculate PID output (control input vector $\mathbf{u} = [N, E, \psi]^T$) for each axis
6. Transform force vector from PID controller to BODY coordinates
7. Perform thrust allocation with the force vector from step 6, and find thrust settings for each thruster
8. Yield outputs to the thrusters according to the results from step 7
9. Repeat from step 1

Since we do not have a model of our USV prototype the parameters in each PID-controller (K_p, K_i og K_d) must be found through testing using the Ziegler-Nichols method or similar. The integration effect from the PID controller is able to regulate the error to 0 over time [2], [10].

Note that in manual mode, controlling the USV with a joystick, the joystick readings are fed directly to the thrust allocation algorithm. Hence, x-y movements of the joystick are are transformed to forces in the horizontal plane and joystick rotation is transformed to rotational torque (control of heading).

4) Thrust Allocation: The thrusters are configured as shown in Fig. 6. In order to transform the force vector

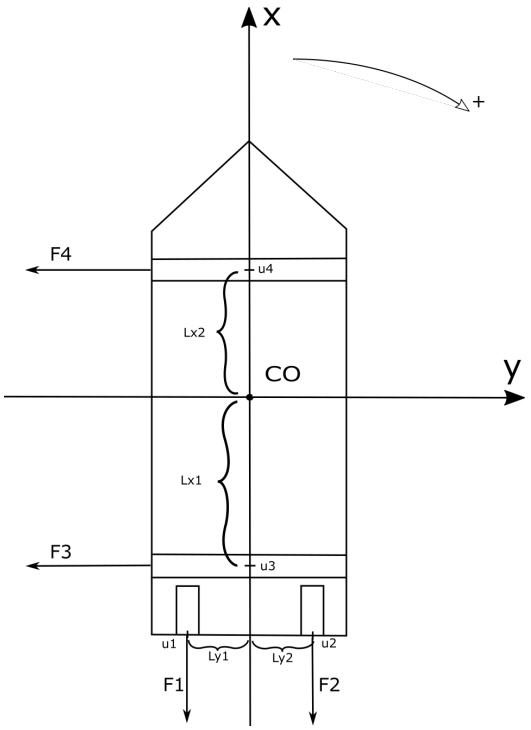

Fig. 6. Thruster configuration.

into appropriate control signals for each thruster, we need a transformation matrix. The desired force vector is defined as $\boldsymbol{\tau}_{\text{ref}} = \begin{bmatrix} X & Y & N \end{bmatrix}^T$, where X and Y are desired forces in the x-direction (forward) and y-direction (sideways), respectively, and N is the desired torque around the z-axis (heading). The forces from each thruster are defined as a vector $\mathbf{u} = \begin{bmatrix} u_1, u_2, u_3, u_4 \end{bmatrix}$. The rank of the system is 4 since we have 4 thrusters.

The thruster forces and torque are related to the desired force vector $\boldsymbol{\tau}_{\text{ref}}$ through the equation

$$\boldsymbol{\tau}_{\text{ref}} = \mathbf{T}\mathbf{u} \tag{7}$$

where $\mathbf{T}$ is a matrix that describes the configuration shown in 6.

Specifically, for u_1–u_4, we get

$$\boldsymbol{\tau} = \begin{bmatrix} 1 \\ 0 \\ L_{y1} \end{bmatrix} u_1 \tag{8}$$

$$\boldsymbol{\tau} = \begin{bmatrix} 1 \\ 0 \\ -L_{y2} \end{bmatrix} u_2 \tag{9}$$

$$\boldsymbol{\tau} = \begin{bmatrix} 0 \\ 1 \\ -L_{x1} \end{bmatrix} u_3 \tag{10}$$

$$\boldsymbol{\tau} = \begin{bmatrix} 0 \\ 1 \\ L_{x2} \end{bmatrix} u_4 \tag{11}$$

where L denote lengths as given by Fig. 6. Combining these equations, we obtain in vector-matrix form

$$\boldsymbol{\tau}_{\text{ref}} = \begin{bmatrix} X \\ Y \\ N \end{bmatrix} = \begin{bmatrix} 1 & 1 & 0 & 0 \\ 0 & 0 & 1 & 1 \\ L_{y1} & -L_{y2} & -L_{x1} & L_{x2} \end{bmatrix} \begin{bmatrix} u_1 \\ u_2 \\ u_3 \\ u_4 \end{bmatrix} = \mathbf{Tu} \tag{12}$$

For our physical prototype, the measured distances were $L_{x1} = 0.8$ m, $L_{x2} = 0.87$ m, and $L_{y1} = L_{y2} = 0.2$ m. The challenge for the thrust allocation algorithm is to find the values for $\mathbf{u}$ that satisfies eq. (12).

5) Optimal Control: Equation eq. (12) describes an underdetermined system since the number of equations are less the the number of unknown control inputs $\mathbf{u}$. Thus, there exists an infinite number of solutions and the system is said to be redundant, as observed previously, since we have 4 thrusters controlling 3 DOF.

One method for selecting an appropriate solution is to use optimisation. In order to find the smallest power requirement and to avoid saturation of the thrusters, the optimisation problem can be defined using linear quadratic constrained control allocation [11]:

$$\begin{aligned} \underset{\mathbf{u},\mathbf{s}}{\text{minimise}} \quad & \mathbf{u}^T\mathbf{W}\mathbf{u} + \mathbf{s}^T\mathbf{Q}\mathbf{s} \\ \text{with constraints} \quad & \mathbf{Tu} = \boldsymbol{\tau}_{ref} + \mathbf{s} \\ & \mathbf{u}_{min} \leq \mathbf{u} \leq \mathbf{u}_{max} \end{aligned} \tag{13}$$

$\mathbf{W}$ is a cost matrix for the control input but since all thrusters are equal we can replace it by the identity matrix. The symbol $\mathbf{s}$ is a slack variable with a corresponding weight matrix $\mathbf{Q}$. The slack variable will allow for cases where $\boldsymbol{\tau}_{\text{ref}}$ cannot be reached by $\mathbf{Tu}$. The condition $\mathbf{u}_{min} \leq \mathbf{u} \leq \mathbf{u}_{max}$ prevents the thrusters from saturation. The constraints $\mathbf{u}_{min}$ and $\mathbf{u}_{max}$ are the minimum and maximum values the thrusters can achieve.

By choosing $\mathbf{Q} \gg \mathbf{W} > \mathbf{0}$ we make sure that the slack variable $\mathbf{s}$ is minimized. Hence, the force vector $\mathbf{Tu}$ becomes as accurate as possible (under the constraints) [11].

The open source library JOptimizer [12] for Java solves problems in the following form by using a primal-dual interior-point algorithm to solve the quadratic optimisation problem:

$$\begin{aligned} \underset{\mathbf{z}}{\text{minimise}} \quad & \mathbf{z}^T\boldsymbol{\Phi}\mathbf{z} \\ \text{with constraints} \quad & \mathbf{A}_1\mathbf{z} = \mathbf{C}_1\mathbf{p} \\ & \mathbf{A}_2\mathbf{z} \leq \mathbf{C}_2\mathbf{p} \end{aligned} \tag{14}$$

A description of this algorithm can be found in [13].

We may transform our optimisation problem in eq. (13) to the form described by eq. (14) for solving using JOptimizer by defining

$$\begin{aligned} \mathbf{p} &= \begin{bmatrix} \boldsymbol{\tau}_{ref}^T & \mathbf{u}_{min}^T & \mathbf{u}_{max}^T \end{bmatrix}^T \\ \text{and} \quad \mathbf{z} &= \begin{bmatrix} \mathbf{u}^T & \mathbf{s}^T \end{bmatrix}^T \end{aligned} \tag{15}$$

and

$$\begin{aligned} \boldsymbol{\Phi} &= \begin{bmatrix} \mathbf{W} & \mathbf{0}_{4\times3} \\ \mathbf{0}_{3\times4} & \mathbf{Q} \end{bmatrix} \\ \mathbf{A}_1 &= \begin{bmatrix} \mathbf{T} & -\mathbf{I}_{3\times3} \end{bmatrix} \\ \mathbf{C}_1 &= \begin{bmatrix} \mathbf{I}_{3\times3} & \mathbf{0}_{3\times8} \end{bmatrix} \\ \mathbf{A}_2 &= \begin{bmatrix} -\mathbf{I}_{4\times4} & \mathbf{0}_{4\times3} \\ \mathbf{I}_{4\times4} & \mathbf{0}_{4\times3} \end{bmatrix} \\ \mathbf{C}_2 &= \begin{bmatrix} \mathbf{0}_{4\times3} & -\mathbf{I}_{4\times4} & \mathbf{0}_{4\times4} \\ \mathbf{0}_{4\times3} & \mathbf{0}_{4\times4} & \mathbf{I}_{4\times4} \end{bmatrix} \end{aligned} \tag{16}$$

When the amount of force each thruster shall deliver has been found, we need to give the correct output to the thruster controller called ESC. The ESC supplied by Blue Robotics for our T200 [6] uses a pulse-width modulated (PWM) signal and the force versus PWM signal is shown in Fig. 7.

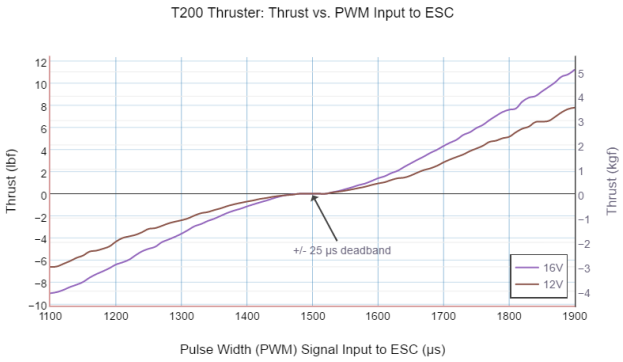

Fig. 7. Force versus PWM input to ESC [6].

We can apply polynomial regression on both sides of PWM at 1500 μs resulting in two equations $y_p(x)$ and $y_n(x)$ for force in positive and negative directions:

$$y_p(x) = 6.8045x^3 - 45.9428x^2 + 183.3807x + 1528.9250 \tag{17}$$

$$y_n(x) = 8.1267x^3 - 53.0778x^2 + 206.7802x + 1466.3682 \tag{18}$$

where y is the PWM value and x is the force in Kgf, and our force in Newton must therefore be multiplied by $\frac{1}{g}$ to get the correct x value.

B. Instrumentation

It is essential for the DP algorithm to have reliable measurements of the vessel's position and heading. For position readings we use the global navigation satellite system (GNSS) and chose a low cost GNSS receiver called Ultimate GPS produced by Adafruit. This receiver supports the European Geostationary Navigation Overlay Service (EGNOS) and Wide Area Augmentation System (WAAS) for European and American differential GPS, respectively, and provides resolution down to ±1 m [14]. Its update frequency is 5 Hz, providing data packets in the National Marine Electronics Association (NMEA) MTK Private Protocol (PMTK) format [15]. To improve sensitivity the GPS was connected to an external antenna.

To get an accurate heading the 9 Degrees of Freedom — Razor IMU from SparkFun was used [16]. This IMU combines a gyroscope with a magnetometer and an accelerometer. The advantage of combining them is that a gyroscope will drift over time due to integration of a bias

and a magnetometer may be used to zero-out the error [17]. In addition to providing an accurate heading the IMU unit also provides acceleration data that could be used in a more advanced DP algorithm. The IMU has an onboard ATmega 328 microcontroller and the user may use the provided firmware or upload his own.

Wind direction and force could also be additional input to an advanced DP algorithm [18] and together with air pressure and humidity these data could be useful for the operator and/or the final application. A weather station [19] and an atmospheric sensor [20] from SparkFun were installed but initial tests showed uneven performance from the wind wane. Since these sensors were not crucial for our DP implementation further work with these sensors is left for future work.

C. Onboard Controller

For the onboard computer we selected the Odroid-XU4 by Hardkernel. The Odroid-XU4 belongs to the class of reduced instruction set computing (RISC) processors and is an advanced RISC machine (ARM). The device implements the eMMC 5.0, USB 3.0, and Gigabit Ethernet interfaces and runs various flavours of Linux (e.g. Ubuntu) or Android as its operating system.

Fig. 8 shows the physical implementation of the overall control system, with the following items as labelled:

1. Odroid XU4 with WiFi-antenna
2. Adafruit Ultimate GPS
3. Razor 9 DOF IMU
4. Arduino microcontrollers
5. Temperature/pressure/humidity sensor
6. Terminals for PWM-signal for thrusters
7. Terminals for 5 VDC og 0 VDC
8. USB hub

Fig. 8. Physical implementation of control system.

A circuit diagram of the control system is shown in Fig. 9.

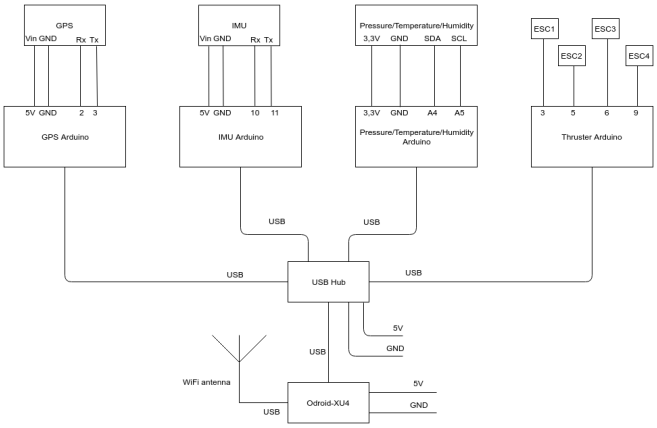

Fig. 9. Circuit diagram of control system.

Fig. 10 shows a diagram of the data flow of the system, both internally and between the vessel and the remote terminal (text in Norwegian).

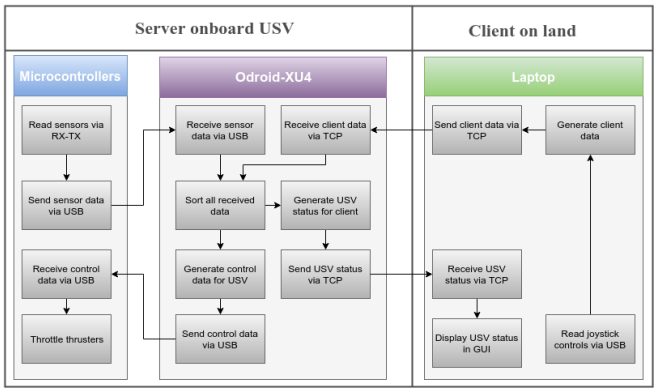

Fig. 10. System data flow diagram.

D. Remote Controller

The operator can control the vessel using a remote terminal with a graphical user interface (GUI). The GUI was made in Java using the Swing library and a screenshot is shown in Fig. 11. Using the interface allows for sending commands to

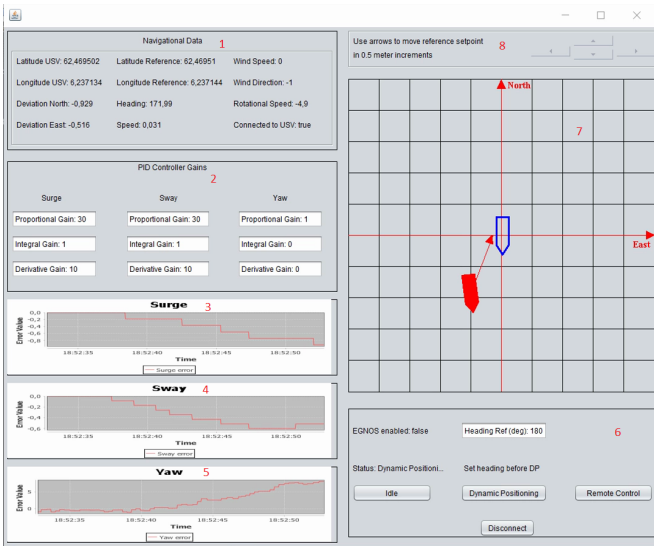

Fig. 11. Graphical user interface (GUI).

the vessel and receiving information, e.g., deviations (errors)

in desired surge, sway, yaw, and position, speed, heading and rotational speed. All communication between the vessel and the remote controller is transmitted via WiFi. Hence, the current operating range of our USV is limited by WiFi range, but it can easily be increased using mobile data coverage like 3G/4G.

Fig. 11 show the USV in DP mode, with the following items as labelled:

1. Panel with navigational data such as GPS position, heading and status of communication links, etc.
2. Panel for PID parameter adjustment
3. Trending of error in N-axis (NED-coordinates)
4. Trending of error in E-axis (NED-coordinates)
5. Trending of error in heading
6. Panel for displaying status (current operational mode) and setting the desired heading, operational mode, and remote control.
7. Graphical display of vessel position and orientation relative to the setpoint in NE coordinates.
8. Panel for setpoint adjustment in 0.5 m increments

IV. Prototype Testing and Results

Speed tests were done by logging GPS data from tests in relocation mode. Rotational speed $\dot{\psi}$ was calculated using numerical derivation of the heading angle logged from the IMU:

$$\dot{\psi} = (\psi - \psi_{\text{previous}})/t_{\text{s}} \tag{19}$$

where the sample time t_{s} is the interval between samples from the IMU. Force was measured using a spring scale type force gauge.

The results are shown in Table I. As can be seen from

TABLE I
MAXIMUM SPEED AND FORCE FOR SURGE, SWAY, AND YAW.

Axis	Maximum speed	Force
Surge, forward	0,6(m/s)	40(N)
Surge, backward	0,5(m/s)	25(N)
Sway, starboard	0,48(m/s)	35(N)
Sway, port	0,56(m/s)	40(N)
Yaw (heading)	$\pm$40(°/s)	-

table, there is little difference between the maximum speed in any direction, ranging from 0.48 m/s to 0.6 m/s. The reason the vessel moves so easily in any direction is that it is has a flat bottom and floats very high in the water. Whilst the the maximum positional speed is quite small, the rotational speed of $\pm 40°$/s makes the vessel very responsive to changes in yaw.

The force readings are in the range of 25–40 N but were difficult to obtain and should only be considered indicative because of oscillating values.

V. Conclusions

We have demonstrated by rapid prototyping of a COTS USV for aqua farm inspection as an example that it is possible to produce a low cost DP platform that can be used for many different applications. The total cost of the prototype (all equipment included) was below 2000 EUR.

Our prototype proved to perform well in some simple quantitative preliminary tests and by qualitative observation during operation (please see our videos on YouTube linked to in Section I).

The prototype has speed limitations due to the size of its thrusters. This will result in the vessel being unable to maintain position if wind or current is above certain thresholds. Hence, for correct thruster dimensioning it will be important to know both the operational requirements (duty/availability ratio) and the ocean current and weather conditions at the locations the vessel will operate in.

VI. Future Work

Our plan for the coming year is to add subsea monitoring, to improve vessel performance, and to add operational features. In order to perform subsea monitoring we will develop a simple low cost tethered ROV and a suitable winch that is heave compensated. In order to make the vessel more streamlined we will replace the low cost COTS boat with a custom-made boat while still aiming and keeping costs at a minimum. We will design our own hull. The new design will allow the thrusters to be integrated into the hull. New thrusters will also be considered in order to operate in more harsh weather conditions. New autonomous operational features will include an autopilot with route planning and waypoints in order to operate out-of-sight and out-of-radio range.

References

[1] S. Corfield and J. Young, "Advances in unmanned marine vehicles," *IET Control Engineering Series*, vol. 69, no. 2008, pp. 313–317, 2008.

[2] T. I. Fossen, *Handbook of Marine Craft Hydrodynamics and Motion Control*. John Wiley & Sons, Ltd, 2011.

[3] Sleipner Motor AS, "Tunnel installation guide," Side-Power Thruster Systems, Tech. Rep. May 2016, 2016. [Online]. Available: \url{https://side-power.com/media/frontend_media/pdf/current_manuals/EBS20_EB90_v1_1_3_2015_LR.pdf}

[4] A. F. Mollard, S. R. Turnock, and D. A. Hudson, *Ship Resistance and Propulsion*. Cambridge University Press, 2013.

[5] J. Holtrop and G. Mennen, "An approximate power prediction method," *International Shipbuilding Progress*, vol. 29, no. 335, pp. 166–170, 1982.

[6] (2016) T200 thruster documentation. [Online]. Available: http://docs.bluerobotics.com/thrusters/t200/#d-model

[7] (2016) Saltwater transom-mount | riptide transom. [Online]. Available: http://www.minnkotamotors.com/Trolling-Motors/Saltwater-Transom-Mount/Riptide-Transom/

[8] (2015) Lecture Notes TTK4190 Guidance and Control of Vehicles. [Online]. Available: http://www.fossen.biz/wiley/Ch2.pdf

[9] A. Sørensen, "A survey of dynamic positioning control systems," *Annual Reviews in Control*, vol. 35, pp. 123–136, 2011.

[10] N. S. Nise, *Control Systems Engineering*, 6th ed. John Wiley & Sons, 2009.

[11] T. I. Fossen and T. A. Johansen, "A survey of control allocation methods for ships and underwater vehicles," in *2006 14th Mediterranean Conference on Control and Automation*, G. Conte and M. Napoletano, Eds., 2006, pp. 1–6.

[12] (2016) Primal-dual interior-point method. [Online]. Available: http://www.joptimizer.com/primalDualMethod.html

[13] S. Boyd and L. Vandenberghe, *Convex Optimization*. Cambridge University Press, 2009.

[14] (2016) Adafruit Ultimate GPS. [Online]. Available: https://cdn-learn.adafruit.com/downloads/pdf/adafruit-ultimate-gps.pdf

[15] (2012) GlobalTop PMTK command packet. [Online]. Available: https://cdn-shop.adafruit.com/datasheets/PMTK_A11.pdf

[16] (2015) Razor 9DOF IMU, Sparkfun. [Online]. Available: https://www.sparkfun.com/products/10736

[17] J. Borenstein, L. Ojeda, and S. Kwanmuang, "Heuristic reduction of gyro drift for personnel tracking systems," *Journal of Navigation*, vol. 62, pp. 41–58, 1 2009. [Online]. Available: http://journals.cambridge.org/article_S0373463308005043

[18] R. Stephens, "Wind feedforward: blowing away the myths," *Marine Technology Society Dynamic Positioning Conference*, 2011.

[19] (2015) Weather meters. [Online]. Available: https://www.sparkfun.com/products/10736

[20] (2015) SparkFun Atmospheric Sensor Breakout - BME280. [Online]. Available: https://www.sparkfun.com/products/13676

AUTHOR BIOGRAPHIES

OTTAR L. OSEN graduated with MSc in Engineering Cybernetics from the Norwegian Institute of Technology in 1991 (NTH, now the Norwegian University of Science and Technology (NTNU)). He is the head of R&D at ICD Software AS and an assistant professor at NTNU in Ålesund. In addition to 10 years in academia he has worked for 15 years as an consultant in the maritime and offshore industry both in Norway and internationally. He has taken part in the engineering phase on several of the large offshore projects on the Norwegian continental shelf. He has broad experience in subsea control systems and SCADA systems in general. His research interests belong to the fields of artificial intelligence, cybernetics, instrumentation, real-time systems, industrial control systems, mechatronics, and modelling and simulation.

ROBIN T. BYE[4] graduated from the University of New South Wales, Sydney with a BE (Honours 1), MEngSc, and a PhD, all in electrical engineering. Dr. Bye began working at NTNU in Ålesund (formerly Aalesund University College) as a researcher in 2008 and has since 2010 been an associate professor in automation engineering. His research interests belong to the fields of artificial intelligence, cybernetics, and neuroengineering.

ALBERT HAVNEGJERDE, **VEGARD KAMSVÅG** and **SVEINUNG LIAVAAG** graduated with a BSc in automation engineering at NTNU in Ålesund in 2016.

[4]www.robinbye.com